

Estimation and Control for Autonomous Coring from a Rover Manipulator

Nicolas Hudson¹, Paul Backes, Matt DiCicco, Max Bajracharya
Jet Propulsion Laboratory, California Institute of Technology
¹nicolas.h.hudson@jpl.nasa.gov

Abstract—A system consisting of a set of estimators and autonomous behaviors has been developed which allows robust coring from a low-mass rover platform, while accommodating for moderate rover slip. A redundant set of sensors, including a force-torque sensor, visual odometry, and accelerometers are used to monitor discrete critical and operational modes, as well as to estimate continuous drill parameters during the coring process. A set of critical failure modes pertinent to shallow coring from a mobile platform is defined, and autonomous behaviors associated with each critical mode are used to maintain nominal coring conditions. Autonomous shallow coring is demonstrated from a low-mass rover using a rotary-percussive coring tool mounted on a 5 degree-of-freedom (DOF) arm. A new architecture of using an arm-stabilized, rotary percussive tool with the robotic arm used to provide the drill z-axis linear feed is validated. Particular attention to hole start using this architecture is addressed. An end-to-end coring sequence is demonstrated, where the rover autonomously detects and then recovers from a series of slip events that exceeded 9 cm total displacement.

TABLE OF CONTENTS

1 INTRODUCTION	1
2 ROTARY PERCUSSIVE CORING WITH ARM STABILIZATION	2
3 SENSORY AND ROBOTIC PLATFORM	4
4 AUTONOMY SYSTEM	6
5 SLIP EXPERIMENTS	7
6 CONCLUSIONS	8
ACKNOWLEDGEMENTS	8
REFERENCES	8
BIOGRAPHY	10

1. INTRODUCTION

A future Mars Sample Return (MSR) mission could utilize a low-mass rover to acquire shallow core samples that could be stored and returned to Earth. Future missions could benefit by enabling drilling or coring from a low-mass rover where the rover might experience modest slippage during the drilling or coring operation. A low-mass rover might be on the order of 200 kg.

The current state-of-the-art in coring or drilling from a planetary rover, represented by the upcoming 2011 Mars Science Laboratory (MSL) mission, assumes that the rover is a rigid platform for the coring tool or drill. MSL uses an arm-mounted manipulator to provide a rigid base for the drill by pressing external stabilizing tines against a surface with a large preload. The drill will then provide its own translational degree-of-freedom (DOF) to control interaction with the rock. It is reasonable to assume that when the rover is heavy enough it will not move during the coring operation, as the case for the MSL mission. This assumption is not reasonable when the rover's mass is low relative to the interaction forces with the environment or when the rover is on a slope where it could possibly slip.

Several other drilling and coring tool designs have been developed for potential future rover and lander missions to Mars. A review of these designs [1], includes arm-mounted rotary-percussive drills such as the Alliance Spacesystems Inc. (ASI) low-force sample acquisition system (LSAS), the arm-mounted rotary-drag Honeybee Corer-Abrader Tool (CAT), and body-mounted tools such as the Honeybee Mini-Corer. So far, limited autonomy has been developed for deploying shallow coring tools on Mars. These hardware systems may have been used (on Earth) with levels of autonomy similar to the Mars Exploration Rover (MER) Rock Abrasion Tool (RAT), which contain limit checks on tool current and contact sensors, and simply decide whether to abort or continue coring or abrading [2]. This level of autonomy might suffice for future missions with frequent input from ground systems, but it will not enable missions with critical failure modes such as rover slip, time-critical missions, or missions with expectations of tool binding [3].

The Integrated Mars Sample and Handling System (IMSAH), architecture has been proposed for potential future Mars sample missions [4]. IMSAH uses an architecture akin to the LSAS tool; a rotary percussive coring tools is mounted on the end of a 5 degree of freedom (DOF) robotic arm, or tool deployment device (TDD). The tool does not contain an active linear feed but instead utilizes a passive spring-based linear feed. The TDD can compress the feed against the target sample site to apply the required weight-on-bit (WOB).

The ability to reliably start a hole using an arm-stabilized coring tool is investigated and validated using two experimental setups. During the IMSAH development process, hole start

¹ 978-1-4244-3888-4/10/\$25.00 ©2010 IEEE.
IEEEAC Paper #1540, Version 2.1, updated 05/01/2010.

was identified as a primary concern. Section 2 details the experiments used to validate the architecture’s ability to conduct hole start procedures.

One goal of the IMSAH architecture is to acquire core samples on slopes while accommodating moderate slip conditions. A second goal is to provide a system capable of fast sample acquisition, acquiring the sample within one Martian sol, without extended input for ground based diagnostics. These goals will require an autonomy system capable of closed loop coring control, diagnosing coring faults, and fault recovery and accommodation for continued coring.

This paper presents a set of estimators and autonomous behaviors, which can robustly estimate coring faults from a low-mass rover and accommodate to enable continued coring. The resulting system is capable of answering two related questions: first, the discrete fault diagnosis of “is the rover slipping?”, and second, the estimation of continuous state “how much has the rover slipped?”. Affirmation of the first question will send the rover into a safety state where the coring tool is stopped. The estimate of slip distance is used to reconfigure the rover to relieve lateral forces on coring tool and to return the rover to a state where coring can continue. The system also utilizes several redundant sets of sensors to provide robustness to any single sensor failure.

The developed system builds upon previous work in drilling autonomy. Of most relevance to coring on low mass rovers and mobile platforms, is work involving slip compensation for arm mounted coring tools [5]. Here, absolute motion visual odometry (AMVO) is used to provide an estimate of rover displacement from the initial coring position, allowing reconfiguration of the rover arm to continue coring during moderate (< 1 cm/min) rover slip. This work was then extended to providing limited slip accommodation on body mounted coring using a translate-pitch mechanism and the MiniCorer tool [6]. Here, both a force torque sensor and AMVO were used to reconfigure the rover during moderate, in plane slip. Both [5] and [6] use MER relevant avionic systems, and technologies that can be deployed on potential rover missions in the near future. Other work on autonomy for drilling has been focused on deep drilling (> 10 m), notably the Drilling Automation for Mars Exploration (DAME) project [3]. Here the deep-drilling process was autonomously monitored for faults, off nominal conditions, and used combination of drill speed, weight on bit, drill torque and drill-string-vibration measured from a laser vibrometers. The DAME system determined faults from a combination of heuristic rules from drill speed torque and WOB, a neural network that monitors vibration, and a high level model based reasoning using the Hybrid Diagnostic Engine (HyDE).

The remainder of this paper is organized as follows: Section 2 discusses the IMSAH drill architecture, and describes and validates hole start using arm-stabilized rotary percussive coring tools. Section 3 describes the sensors used to monitor and

diagnose the coring process, and details the specific FIDO [7] rover, hardware, and the software architecture used. Section 4 describes the estimation algorithm and autonomy system. Section 5 shows an autonomous end-to-end coring test, where the system drills to full depth (5cm) while accommodating up to 9 cm of rover slip.

2. ROTARY PERCUSSIVE CORING WITH ARM STABILIZATION

The IMSAH architecture [?] currently assumes a rotary percussive coring tool arm-mounted coring tool. The tool is assumed to be light weight (< 5 kg) and does not contain an active linear feed. The tool is stabilized using the arm and does not contain any external stabilizers or tines. This is different than the current 2011 MSL mission architecture. MSL uses an arm-mounted manipulator to provide a rigid base for the drill by pressing external stabilizing tines against surface with a large preload, and the drill provides its own translational DOF to apply Weight-on-Bit (WOB) against the rock. Because the IMSAH architecture does not utilize external stabilizers for drilling, the mass of the tool can be further reduced by removing the active linear feed, and replacing it with a passive spring system that can be preloaded against the rock to provide the appropriate WOB.

The IMSAH architecture is currently represented by mounting a stripped-down, low-weight (1.5kg) Bosch rotary hammer drill (11536C) on the end of a 5-DOF arm on a FIDO rover (Figure 1).

Linear Feed and Coring Cycle

To reduce power consumption, it is assumed that the coring tool will not operate while the arm is moving. Currently it is assumed that the drill may consume up to 65 W while coring, and that this potentially could exceed a future low-mass rover’s ability to operate the arm while coring. This necessitates a cyclic coring architecture where the coring bit is first preloaded against the rock to achieve a desired WOB, then the arm is locked using brakes, and then the coring tool is turned on. As the coring tool operates, a spring driven (or equivalent) passive linear feed is used to push the tool forward as rock is removed. Once the coring bit has penetrated into the rock and the WOB decreases past a set-point, the tool is stopped and the robotic arm is used to compress the passive linear feed and reapply WOB. The coring cycle and passive linear feed device is shown in Figure 2.

Hole Start

Hole start was identified as a critical period of the coring operation. This section describes the experiments that validate hole start can be robustly performed using an arm-mounted, arm-stabilized, rotary-percussive coring tool. Note that previous work had shown success with this architecture using the LSAS tool on a compliant arm [5], but this was done with a low powered (15W) tool, and the arm and tool could operate at the same time. The concern over hole start was based on

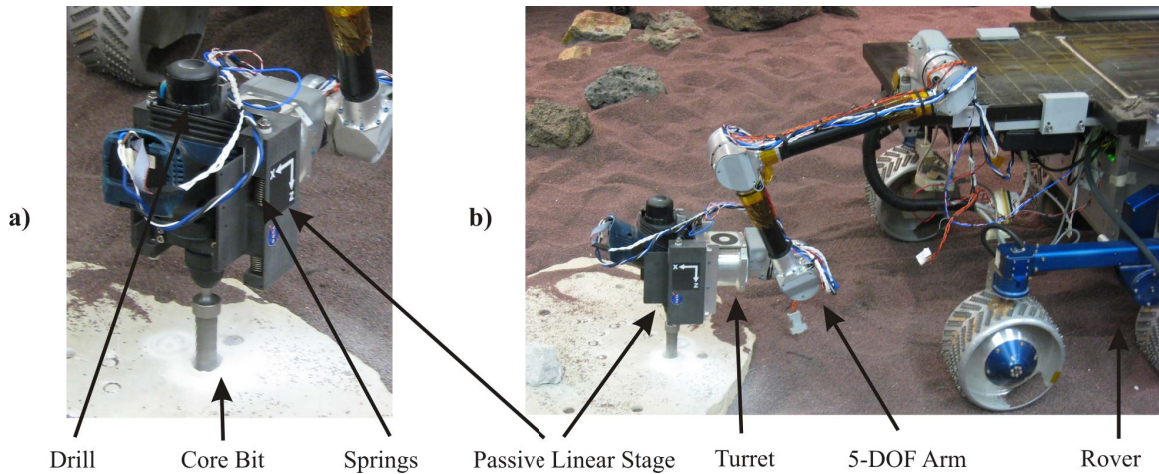


Figure 1. Arm-mounted rotary-percussive coring tool. Testing was done using a 5-DOF arm mounted on a FIDO rover. A Bosch 11536C drill was stripped down and used as a representative coring tool. The rover is shown coring into a flat limestone rock.

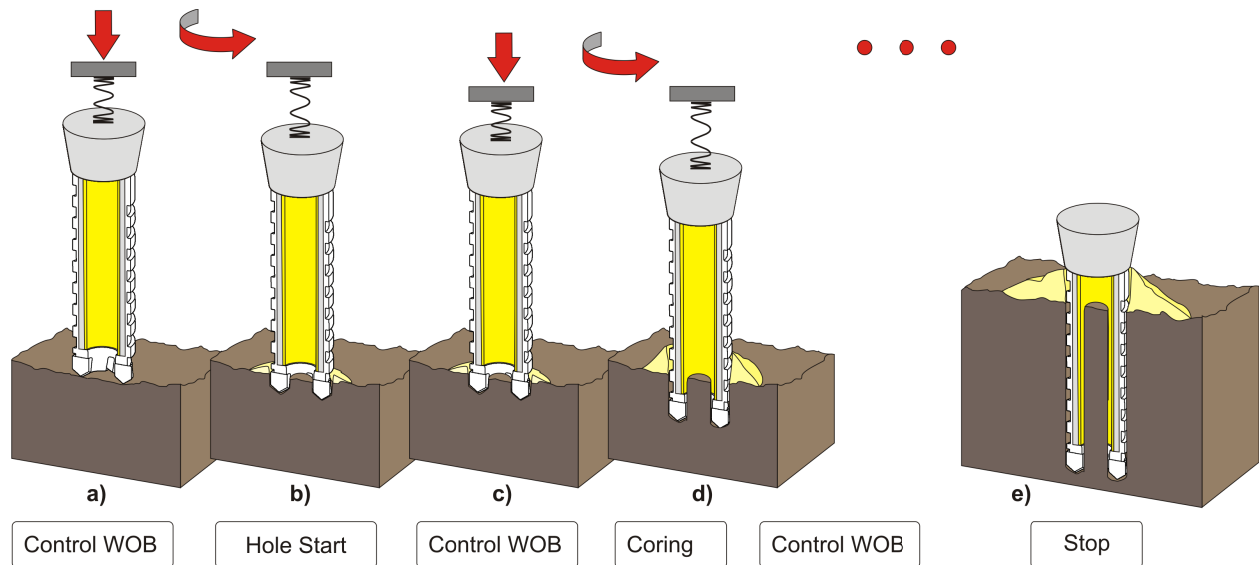


Figure 2. The IMSAH coring Process: The coring tool and the arm do not operate at the same time. First the arm is moved to apply correct WOB. Second the arm is locked using brakes, and the coring tool is turned on. This process continues until the desired coring depth has been reached.

experience using rotary-drag tools on compliant stands and trying to start a core with commercial rotary percussive tool held by hand. Typically the drill can 'walk' along the surface. With rotary-drag tools this is due to the high weight on bit, and lateral forces caused by drill torque and uneven tooth contact. Rotary-drag coring tools necessitate either a centering bit, or a highly rigid mounting. Starting a core with a hand-held rotary-percussive tool also typically results in bit walk, the human arm cannot provide the a reliable centering force to keep the drill centered.

The advantage of using a robotic arm over a human one, is that the end effector of the robotic tool deployment device (TDD) is essentially a spring mass damper system. This means that once the coring tool is disturbed from its initial

point of contact with the rock, the spring system will provide an instantaneous restoring force back to the initial contact point. When using a rotary percussive tool, the percussion will break the rock beneath the bit tooth, or bounce the bit upwards reducing the lateral force on the bit due to uneven tooth contact.

Three parameters were initially assumed as important in successfully starting a hole: First, the impact energy of the tool; it was assumed that this would have to be large enough so the drill operated in a rotary-percussive, instead of pure rotary manner. Second, the compliance of the arm; it was assumed that above a certain compliance level the restoring force would be too low to re-center the tool. Third, the weight-on-bit (WOB) was assumed to be an important pa-

Table 1. Approximate compliance of Arm testbed, test rover ('Pluto') in two different configurations and a comparison to the MER IDD

platform	compliance m/N		
	x	y	z
MER IDD	1e-4	2e-4	3e-4
Test stand	1.15e-4	3.9e-4	4.2e-4
Pluto 1	1.0e-4	2.1e-4	2.7e-4
Pluto 2	5.4e-5	3.5e-4	5.2e-4

parameter, as with excessive downward force applied to the bit, the lateral forces on the tool would never be relieved.

The Bosch 11536C drill was used to test hole start. The rotational speed and impact energy of this drill are coupled, and cannot be varied independently. To test hole start a rotation speed of up to 300 RPM was used, which corresponds to approximately 0.3 J per impact with 3.2 impacts per rotation. The Bosch drill took an average of 78 W at 300 RPM during coring in basalt. This drill is working below its optimal working range, as it is intended to operate at higher rpm. A corresponding flight tool would potentially have more impact energy for the same rate of rotation, and is likely to consume less power at the same output levels due to the large amount of energy required to just turn the Bosch at this speed.

The nominal weight-on-bit for hole start was varied between 20 N and 50 N. Less WOB could not be used as the Bosch tool required a certain minimum preload to guarantee that the percussive hammer mechanism would engage with the bit. Most hole start tests took place at 20N, but were increased to 50 N with success.

It was assumed that any future mission that utilizes arm-stabilized coring tool would deploy an arm at least as stiff as the MER IDD. To test the robustness of hole start to arm compliance, a test stand (Fig. 3) was built. This test stand was built to represent a worse-than-typical MER IDD deployment configuration. The approximate stiffness of the MER IDD was calculated using the parameters in [8], with arm angles $\theta = [0, 20, -70, -40, 0]$, and is shown in Table 1. The compliant test stand, shown in Figure 3, is more compliant than the calculated MER IDD. For comparison, Table 1 also shows the measured compliance of the research rover and arm setup used in this paper. The compliance of the rover and arm is highly dependent on the configuration used.

A total of 16 tests were conducted using both limestone and saddleback basalt at 20 N preload and 300 RPM, on the flexible drill setup (Figure 3). The angle between the rock surface and the coring bit was varied up to 15 degrees off-normal for tests. Every test successfully started a hole in both kinds of rock. A trial with large (7.8 N) residual lateral forces after hole start is shown in Figure 4. An amplified FT sensor (ATI Gamma) was used to collect force data at 1 KHz for compliant test stand trials. Note that all later tests conducted on

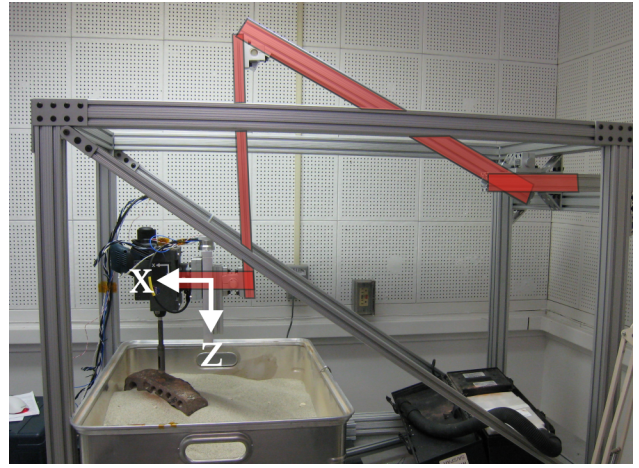


Figure 3. A Compliance test stand used to validate hole start. The test stand was designed to be more compliant than the MER IDD. The compliance of the stand was measured by deflecting the stand in several directions and magnitudes with a force sensor and measuring the deflection with a dial gage.

the FIDO rover (Sec. 5) use an un-amplified force torque (FT) sensor which has to be heavily filtered due to EM noise from the drill and arm motors. A histogram of residual lateral forces after hole start is shown in Figure 5. This histogram contains 5 limestone tests and 11 saddleback basalt tests. Three of the trials conducted with saddleback basalt had the coring bit at an off-normal angle of 15 degrees to the rock surface, two of which make up the largest residual values (7.8 and 11.2 N). There was some concern that with the 15 degree off-normal trials, the results may not be representative complications with the standard SDS chuck used on the Bosch Drill. The SDS chuck allows the bit to slide over a small range in the drill axis direction. Unless the bit is preloaded against the back of the SDS chuck, little percussive energy is transmitted to the bit. With the large angle between the bit axis and rock normal, the compliant stand could allow the bit to 'jump out' of engagement with chuck, even if preloaded.

While all hole start tests were successful, there exists the possibility that induced lateral forces need to be accommodated by moving the arm to conduct successful coring operations. Section 4 discusses a method using the force-torque sensor to relieve lateral bit forces. Note that it is expected that any future deployed system will probably use a stiffer arm, and a greater percussive energy to rotary speed ratio. This will likely further reduce any induced residual forces.

3. SENSORY AND ROBOTIC PLATFORM

This section gives a brief description of the sensors, robotic hardware and software used in to develop and demonstrate robust coring from a light weight rover platform.

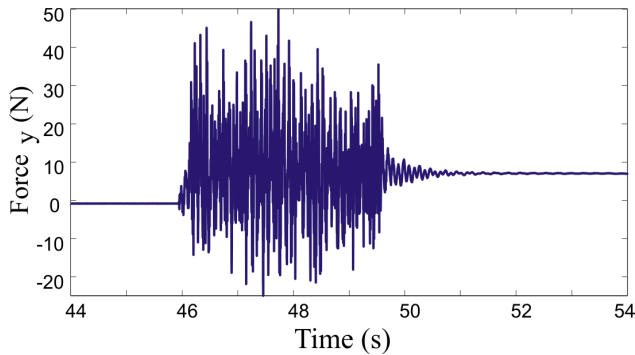


Figure 4. Forces on the drill bit during hole start in the y-axis for a saddleback basalt test at 15 degrees to surface normal.

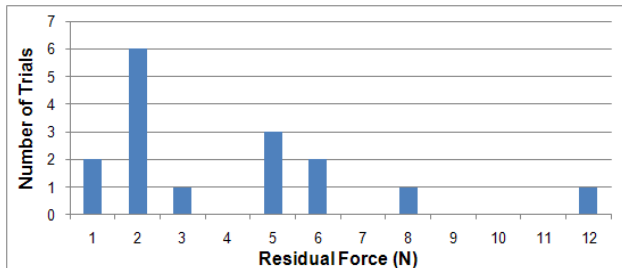


Figure 5. Residual Forces after hole start with compliant test stand. Note that the largest residual force values may not be representative due to complications of the utilized SDS chuck.

Robotic System

Coring tests from a light weight rover were conducted on a FIDO type research Rover at JPL called "Pluto". This rover contains two Mini-ITX form factor motherboards equipped with a 2.5GHz Intel Core2 Duo processor. The two computer approach allows for one machine to focus purely on the vision processing to achieve the visual odometry (VO) frame rates required. Motor control was performed with a set of ElmoMC motor controllers talking on a CAN bus and connected to the main control computer with a CAN to USB converter. Coring and force-control loops were run at 10 Hz. Sensory and motor processes were run at higher rates.

Sensors

A set of sensors were used to monitor the coring process, detect off-nominal coring states, and provide inputs for re-configuring the rover to accommodate rover slip or bit walk. The primary sensors used were a force-torque (FT) sensor, accelerometers, and visual odometry. In addition, measurements of motor velocities, currents, and vehicle IMU data were available.

Force Torque (FT) Sensor

A 6 degree-of-freedom force torque sensor is incorporated into the turret of the TDD (Figure 1), and is used to detect rover slip and for force servoing to realign the coring bit with the hole. In Section 4 an algorithm is described which uses

the force sensor preload the bit to the correct WOB, and can also accommodate induced forces from core bit misalignment or rover slip.

The sensor used is a ATI Industrial Automation Mini45. This sensor has two primary limitations. First, the sensor is not amplified at the sensor, and picks up large amounts of EM noise, in particular when the Bosch Drill is operational. To produce a useful signal, the sensor is digitally filtered at 1000 Hz, using a 15th order Butter worth filter with a cut-off at 5Hz. Second, as calibrated, the sensor saturates at 5 Nm of torque about the x,y, or z axis. While this allows for more precise measurements in near-nominal operation conditions, it has the unfortunate implication that moderate (< 50 N) lateral side loads on the bit can cause sensor saturation. The nominal offset of the bit tip from the FT sensor is greater than 10 cm, meaning that a 50 N load on the bit induces a > 5 Nm torque at the sensor. The sensor itself will not be damaged in these conditions, and is rated up to 110 Nm, but once the sensor saturates the readings are no longer reliable and cannot be used.

Using experimentally gathered stiffness data, it is possible that a moderate slip of 0.5 cm can induce a 50N load on the bit. This assumes a compliance of $1e-4$ N/m from Table 1.

Absolute Motion Visual Odometry

The absolute position of the rover during slip was measured directly by using Absolute Motion Visual Odometry (AMVO), which is a form of stereo camera motion estimation [5]. AMVO was designed to measure the six degrees of freedom (DOF) of motion of a rover for small motions of the vehicle (less than about 50 cm). We use this technique to accurately detect and measure the slippage that a rover undergoes while coring a sample from a rock in its environment. AMVO uses the same algorithm as visual odometry (VO) [9], [10] but it uses the concept of a key pair to avoid the measurement drift associated with VO. Specifically it measures the (6-DOF) displacement from the initial rover frame R_i to the current rover frame R_k , as depicted in Figure 6. AMVO is also used for repositioning the arm when the force torque sensor has an operational fault.

AMVO was performed on the vehicle's 1024x786 (but makes use of image pyramiding) grayscale body-mounted "haz-cams", which have an approximately 110 degree diagonal field-of-view. AMVO as a background process at approximately 7 Hz.

Accelerometers

Accelerometer signals are used to detect off-nominal coring conditions. A tri-axis accelerometer is mounted on the TDD turret and a single-axis accelerometer is mounted directly to the drill body. For all experiments in this paper, the z-axis accelerometer on the turret is used.

The accelerometers are connected to a National Instruments NIUSB-9233 device. This device acquires samples at 2kHz, and automatically low-pass filters at the Nyquist frequency. The device is set to acquire and store 512 data points in a buffer, at which time the data is read as a block by the accelerometer software process. The accelerometer process then windows the data with a Hamming window, and estimates the power-spectral-density (PSD) using a single sided FFT. The 257 PSD data points are sent to the coring process approximately every 1/4 second.

Accelerometers may prove to be an easily flight implementable sensor. The off-the-shelf device (PCB 352C67) used in this experiment can already operate down to -54 C, withstand large amounts of shock, and are insensitive to EM noise.

4. AUTONOMY SYSTEM

The autonomy system is formed around a set of discrete operational modes. A set of estimators are used to switch the system between discrete modes in response to external disturbances such as rover slip. For convenience the coring process can be grouped into five high level states S_1, \dots, S_5 :

- S_1 Deployment to Sample Surface
- S_2 Coring Tool Operational
- S_3 Force/WOB Realignment
- S_4 Visual Servoing Realignment
- S_5 Coring Tool Extraction

A nominal set of state executions was previously depicted in Figure 2. Here the system will deploy to the rock surface and apply a pre-load to the correct WOB (S_1), then will lock the joints on the arm (TDD) and rotate the coring tool at a constant velocity (S_2). Once the WOB drops below a set-point, the system will stop the tool, and use force servoing to reapply preload to maintain the nominal WOB set-point (S_3). States $S_2 \leftrightarrow S_3$ are repeated until the maximum drill depth is exceeded, when the system then extracts the coring tool (S_5).

If critical conditions like rover slip occur, the system must automatically stop the coring tool and start using force realignment to recenter the coring tool and accommodate any induced lateral forces on the bit. Because rover slip can occur during coring while the arm is locked, as estimator is required to detect slip. During larger displacement or fast slip events (where the controller cannot accommodate fast enough to prevent large side loads), the force sensor may saturate due to lateral loads (at $\approx 50N$). In this case the system must automatically switch into a visual servoing mode (S_4) to realign and reduced the forces such that force servoing (S_3) can be used again.

The remainder of this section will describe the force/visual servoing algorithms and the estimators used to detect slip.

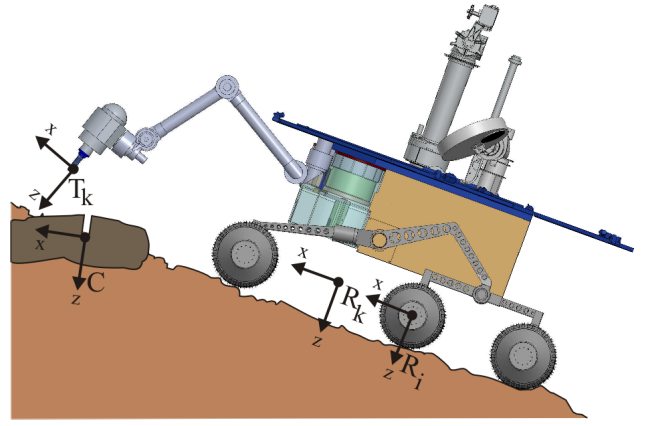


Figure 6. A pictorial representation of relative frames relating to sensor measurements and off-nominal coring conditions. R_i is the *Initial Rover Frame*, or the pose of the rover body at the initiation of the coring process. R_k is the *Current Rover Frame*, or the pose of the rover body at the current time. The *Tool Frame* T_k depends on the configuration and deflection of the tool deployment device. The *Coring Frame* C is the position of the core hole, with the z axis in the down-hole direction.

Force Realignment Algorithm

The force based realignment control strategy is based on previous work of [5]. However, instead of using only the FT sensor to control WOB, it can now be used to compensate for slip as well.

The FT sensor can estimate the transform $D(k)$ from the current tool frame T_k at control step k to the core frame C using the current forces $F(k)$ on the rover manipulator. An approximate model of the rover manipulator gives a spring constant $K(\theta)$ as a function of joint angles, θ . The transform can then be estimated using the stiffness: $D(k) = K(\theta)^{-1}F(k)$. Note that the force $F(k)$ is offset in the z -axis ($F_z(k) = f_z - f_{WOB}$) is used to control around the desired WOB set-point (f_{WOB}).

We denote the homogeneous transform from frame A to frame B as H_A^B .

The Force Realignment Algorithm is initialized by setting the initial tool frame T_i to the current tool frame T_k . At every time step, the current tool frame is moved with respect to the initial tool frame using a small percentage (α) of the estimated displacement $D(k)$:

$$H_{T_k}^{T_i} = H_{T_{k-1}}^{T_i} \alpha D(k) \quad (1)$$

The current to initial tool transform $H_{T_k}^{T_i}$ is converted into rover coordinates:

$$H_{T_k}^{R_k} = H_{R_k}^{R_i} H_{T_i}^{R_i} H_{T_k}^{T_i} \quad (2)$$

Note that when using pure force control, the transform $H_{R_k}^{R_i}$ is set to identity. Currently, the force control algorithm does not

directly estimate displacement in the rover frame, but only in the tool frame. Future work will improve this control strategy, and use this method to incorporate both FT and AMVO sensors at all control steps.

$H_{T_k}^{R_k}$ is computed at each time step, and fed into the inverse kinematics to recover the desired joint angles $\theta(k)$. Force control (1-2) is run at 10Hz. Tracking the joint angles is done off-board the main CPU on the ElmoMC drivers at a much higher inner loop controller (sample rate of 2.75 KHz with a bandwidth of ≈ 80 Hz).

Visual Realignment Algorithm

AMVO gives an estimate of the transform from the starting rover frame to the current rover frame (direct measure of slip) $H_{R_i}^{R_k}$. In circumstances where the force sensor saturates, AMVO can be used to accommodate slip, and hence relieve induced forces, allowing a return to pure force control. This visual alignment algorithm is similar to previous work in [5] where AMVO was exclusively to control lateral slip.

The rover to tool frame transform can now be computed with:

$$H_{T_k}^{R_k} = H_{R_i}^{R_k} H_{T_i}^{R_i} H_{T_k}^{T_i} \quad (3)$$

where $H_{R_i}^{R_k}$ is estimated from AMVO, and $H_{T_k}^{T_i} = H_{T_{k-1}}^{T_i}$ is kept from the force control algorithm. When returning to the force control algorithm, the last transform $H_{R_i}^{R_k}$ is kept to ensure a smooth transition between controllers.

Accelerometer Based Slip Detection

A computationally efficient strategy was taken to create a slip estimator based on accelerometer data. The power spectral density (PSD) data is estimated by an external accelerometer process (Section 3), and is analyzed approximately every 1/4 of a second by the coring process.

To create a training data set, the robot arm was commanded to move laterally while coring to induce side loads. The lateral force on the drill was recorded. Using a single accelerometer the power spectral density was computed. Principle component analysis (PCA) was conducted on the log of the PSD of several training trials. The first principle component of the log(PSD) was shown to have a large degree of correspondence to the induced lateral side loads on the bit, making it a suitable detector for slip (Figure 7). To create a slip detector, the first principle component was modeled as a mixture of Gaussians belonging to either a *slip-class* (defined as when absolute side load force exceeded 5 N) or a otherwise as a *nominal-class*. Figure 7 shows a training data trial used in the determination of the PCA.

The first principle component can easily be computed on new data in real time by convolving the first eigenvector from PCA with the log(PSD) data at every time step. The probability of slip is then defined as the probability of belonging to the *slip-class* model conditioned on the two classes.

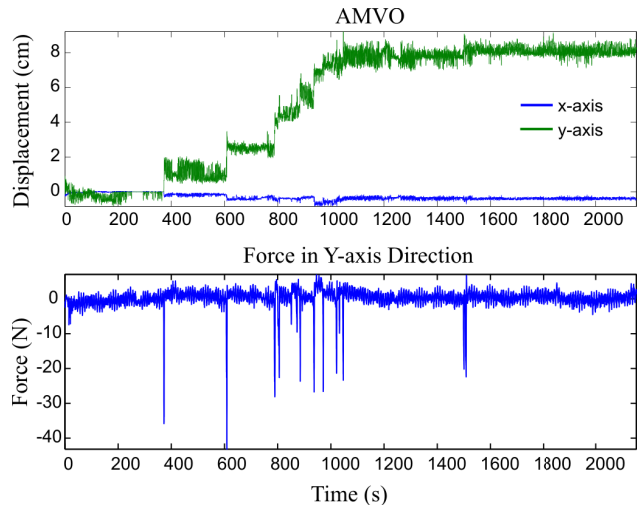


Figure 8. Example of a complete sample acquisition process. The system cored a full depth 5cm hole into Saddleback Basalt in approximately 34 min while accommodating a total of approximately 9cm slip.

Slip Check Algorithm

In general it is advantageous to utilize several redundant sensors to estimating when slip has occurred. To increase robustness, AMVO, the FT sensor, and the accelerometer based detectors are all utilized to detect slip. In this paper, a simple strategy is used to determine slip: if any of the sensors detect slip, the system is put into a safety state. While this strategy will produce more false positives than a consensus algorithm, the increased sensitivity to slip detection and invariance to a single sensor failure was desired. Both the FT sensor and AMVO sensor used simple threshold values to estimate if slip had occurred. Using the accelerometer based detector, a slip state was declared if $P(\text{slip}) > 0.5$.

5. SLIP EXPERIMENTS

The developed autonomous coring algorithms and rover system discussed in this paper have been used to demonstrate robust coring while accommodating slip in several sandbox trials. Coring has been conducted in both Saddleback basalt and limestone rocks successfully. A trial where the rover acquired a full depth (5cm) core into Saddleback is presented here. During the test slip was simulated by pulling on the rover wheels, inducing a total of approximately 9cm displacement from the initial rover position.

The rover's induced slip is shown by the displacement from its initial position as recorded by AMVO in Figure 8. The rover autonomously recovered from all slip events during the coring process, and accommodated to acquire a full depth core. The lateral force on the core bit is also shown in Figure 8, where it is shown that the system was capable of relieving the induced lateral forces from slip events and maintained near-zero lateral forces during the coring process. The system did switch from force based accommodation to AMVO

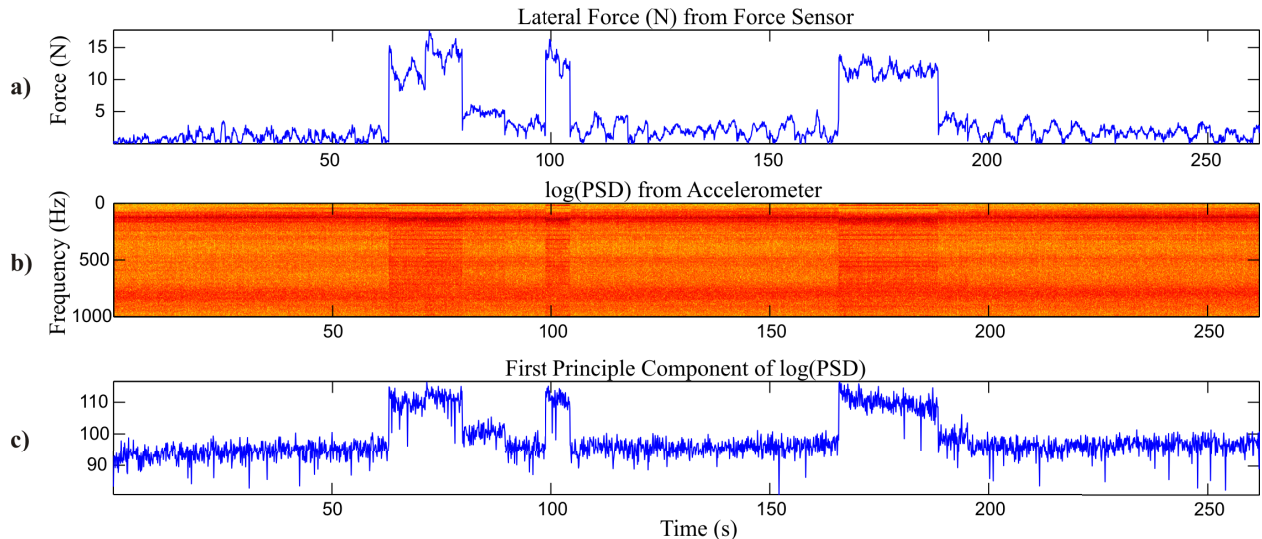


Figure 7. A training data set for accelerometer based slip detection. a) The lateral force exerted on the bit while coring. b) The log of the power spectral density (PSD) of the accelerometer signal. c) The first principle component of the log(PSD) data. The large degree of correspondence between the first component to the induced lateral side loads on the bit make it an excellent detector for slip.

based control due to sensor saturation at around the 600 second mark. This period of time corresponds to a very sudden 1.5 cm slip event, creating large ($> 40\text{N}$) side load on the bit which saturated the FT sensor. Slip was detected and the AMVO based control algorithm returned the rover to a pose where the FT sensor could again be used.

A subset of the trial is shown in more detail in Figure 9. Here AMVO, force and accelerometer based slip detection are shown in conjunction with corresponding operational modes (S_1, \dots, S_5) of the rover. This subset of the trial was chosen to show both periods of time where the rover stopped coring to maintain it's WOB due to the normal coring process, and also periods where force accommodation was entered due to a detected slip event. Note that the accelerometers only provide information about slip while the coring tool is on. All three sensors, AMVO, FT and the accelerometers, provided sufficient information to detect slip. Relatively large thresholds on the FT and AMVO based slip detectors were used.

At the end of the coring process, the drill was extracted linearly along the tool frame z-axis, shown in Figure 10. The robotic arm was then moved back to its original joint angles where it first made contact with the rock to demonstrate the total displacement of slip undergone during the trial.

6. CONCLUSIONS

An autonomy system consisting of a set of estimators and accommodation behaviors was developed and demonstrated to show robust coring from a low mass rover platform while undergoing rover slip and bit misalignment. The system currently uses a set of three sensors: Absolute Motion Visual Odometry, a 6-DOF force-torque sensor and an accelerometer to monitor and automate the coring process. The use

of multiple sensors makes the system more robust to a failure of any single sensory system. The demonstrated coring architecture using an arm-stabilized rotary percussive tool reliably started hole and collect cores in both unfinished saddleback basalt and limestone, and was invariant to moderate (< 15 deg) misalignment between the surface normal of the rock and the tool axis. Future work will continue to utilize more sensory systems including an inertial measurement unit, and drill speed and current to detect and accommodate slip. Methods to probabilistically incorporate all sensory measurements are also being investigated.

ACKNOWLEDGMENTS

The research described in this publication was carried out at the Jet Propulsion Laboratory, California Institute of Technology, under a contract with the National Aeronautics and Space Administration.

REFERENCES

- [1] K. Zacny, Y. Bar-Cohen, M. Brennan, G. Briggs, G. Cooper, K. Davis, B. Dolgin, D. Glaser, B. Glass, S. Gorevan, J. Guerrero, C. McKay, G. Paulsen, S. Stanley, and C. Stoker, "Drilling systems for extraterrestrial subsurface exploration." *Astrobiology*, vol. 8(3), pp. 665–706, 2008.
- [2] S. Mukherjee, P. Bartlett, B. Glass, J. Guerrero, and S. Stanley, "Technologies for exploring the martian subsurface," in *IEEE Aerospace Conference*, 2006.
- [3] B. Glass, H. Cannon, M. Branson, S. Hanagud, and G. Paulsen, "DAME: Planetary-prototype drilling automation," *Astrobiology*, vol. 8(3), pp. 653–664, 2008.

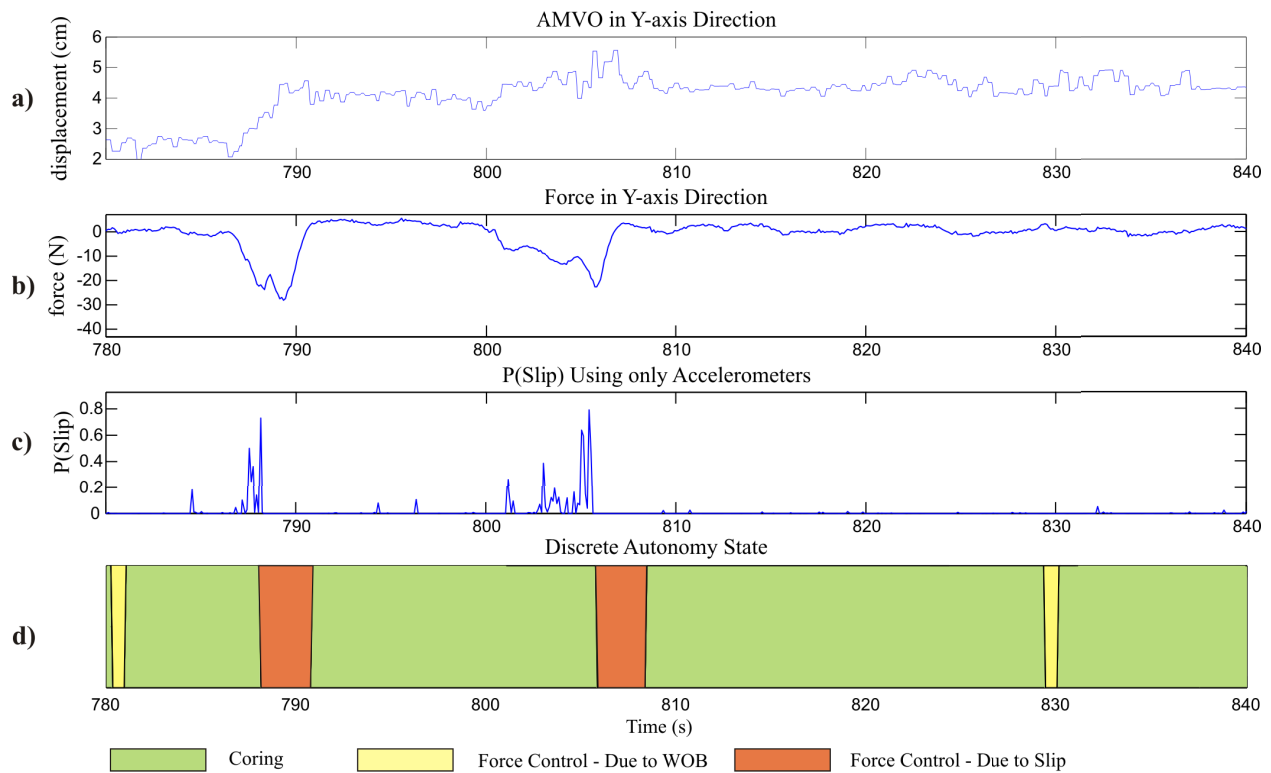


Figure 9. A subset of the coring trial. a) Displacement of the rover from its initial position from AMVO measurements in the rover y-axis. b) Lateral forces exerted on the coring bit. c) The probability of slip using the accelerometer based method. d) The discrete operational state of the autonomy system.

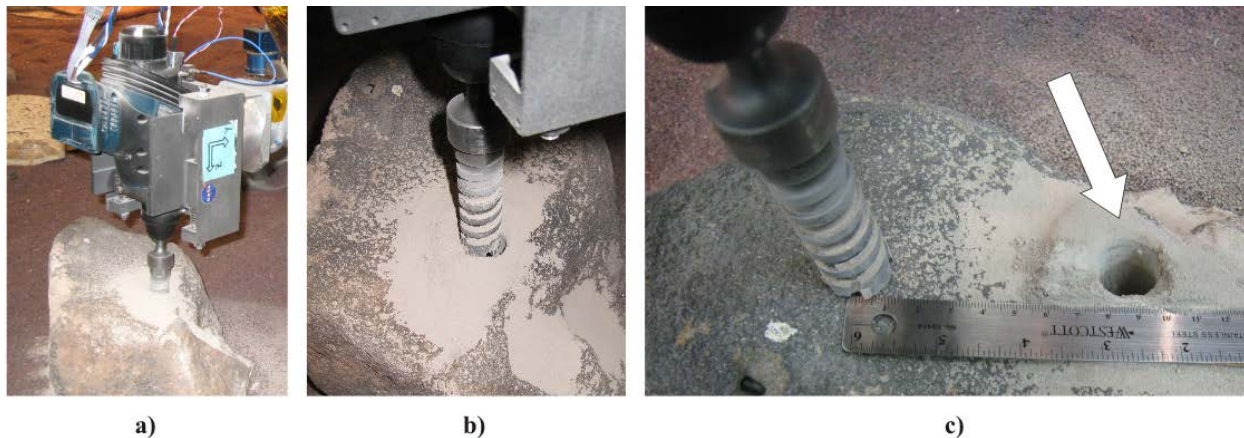


Figure 10. Photos of Drill Bit: a) After drilling 5cm. b) Extraction along drill axis, c) Returned to start position defined by the original joint angles of the arm.

[4] P. Backes, R. Lindemann, and C. Collins, "An integrated coring and caching concept," in *IEEE Aerospace Conference*, 2010.

[5] P. Backes, D. Helmick, M. Bajracharya, O. Khatib, V. Padois, and J. Warren, "Results of coring from a low mass rover," in *IEEE Aerospace Conference*, March 2008, pp. 1–7.

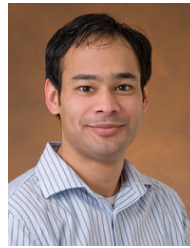
[6] N. Hudson, P. Younse, P. Backes, and M. Bajracharya, "Rover reconfiguration for body-mounted coring with slip," in *Aerospace conference, 2009 IEEE*, March 2009, pp. 1–7.

[7] P. S. Schenker, E. T. Baumgartner, P. G. Backes, H. Agazarian, L. Dorsky, J. S. Norris, T. L. Huntsberger, Y. Cheng, A. Trebi-Ollennu, M. S. Garrett, B. A. Kennedy, A. J. Ganino, R. E. Arvidson, and S. Squyres, "FIDO: a field integrated design & operations rover formars surface exploration," in *Proceeding of the 6th International Symposium on Artificial Intelligence and Robotics & Automation in Space*, June 18-22 2001.

[8] E. Baumgartner, R. Bonitz, J. Melko, L. Shiraishi, and

P. Chris Leger, "The mars exploration rover instrument positioning system," in *Aerospace Conference, 2005 IEEE*, March 2005, pp. 1–19.

- [9] M. Maimone, Y. Cheng, and L. Matthies, "Two years of visual odometry on the mars exploration rovers," *Journal of Field Robotics*, vol. 24(3), Special Issue on Space Robotics, pp. 169–186, 2007.
- [10] A. Howard, "Real-time stereo visual odometry for autonomous ground vehicles," in *IEEE/RSJ International Conference on Intelligent Robots and Systems*, 2008, pp. 3946–3952.



Max Bajracharya is a senior member of the Mobility and Manipulation Group at the Jet Propulsion Laboratory, Pasadena, CA. His research includes vision-based tracking, manipulation, navigation, and pose estimation for robotic vehicles. He is currently the task lead for research tasks focusing on learning terrain classification and pedestrian detection. Max received his Bachelors and Masters degrees in computer science and electrical engineering from MIT in 2001.

BIOGRAPHY



Nicolas Hudson, PhD is a member of the Mobility and Manipulation Group at Jet Propulsion Laboratory. He received his Masters in mechanical engineering and PhD from California Institute of Technology in 2004 and 2008, respectively, and a Bachelor in Engineering degree from the University of Canterbury, Christchurch, New Zealand, in 2002. He received the Sir William Pickering Fellowship at the California Institute of Technology and the Ian McMillan Prize and C.S. McCully Scholarship at the University of Canterbury. His primary area of research at JPL is robotics autonomy for sample acquisition.



Paul Backes, PhD is the group supervisor of the Mobility and Manipulation Group at the Jet Propulsion Laboratory, California Institute of Technology, where he has been since 1987. He received the BSME degree from U.C. Berkeley in 1982 and PhD in 1987 in mechanical engineering from Purdue University. Dr. Backes received the 1993 NASA Exceptional Engineering Achievement Medal for his contributions to space telerobotics, 1998 JPL Award for Excellence, 1998 NASA Software of the Year Award Sole Runner-up, 2004 NASA Software of the Year Award, and 2008 IEEE Robotics and Automation Award. He has served as an associate editor of the IEEE Robotics and Automation Society Magazine.



Matt DiCicco has been a member of the Mobility and Manipulation Group at JPL since June 2005. He received a masters degree from MIT in 2005 where he studied high power robotic manipulators for the Navy and a bachelors degree from Carnegie Mellon in 2003 where he work on medical robotics to aid the disabled. At JPL, Matt has worked on numerous research tasks related to manipulator control. His is currently developing control software for Mars sample return research activities and simulation software for lunar surface operations activities.